Theoretical Vibration and Flutter Studies of Point Supported Panels

E. H. DOWELL*
Princeton University, Princeton, N. J.

Theoretical structural models are developed for point supported panels typical of proposed space shuttle construction which are suitable for vibration and flutter analyses. Representative results for panel natural frequencies and flutter boundaries are presented. These are obtained using quasi-steady aerodynamics which ignore the aerodynamic boundary layer. It is shown for a proposed space shuttle design that the supports must be modeled as points rather than as continuous supports in order to obtain accurate results and that simply increasing the number of supports may not be beneficial as far as flutter is concerned.

Nomenclature

a	= plate length
b	= plate width
D,D_x,D_y,D_1,D_{xy}	= plate stiffnesses
E	= modulus of elasticity
F	= Airy stress function
h	= plate thickness
K	= $\omega(\rho_m h a^4/D)^{1/2}$
K_{mn}	= generalized stiffness
M	= Mach number
M_{mn}	= generalized mass
N	= stress resultant
p	= aerodynamic pressure
Q_n	= generalized force
$q;q_n$	= $\rho U^2/2$; generalized coordinate
t	= time
U	= mean flow velocity over panel; also strain energy
u,v,w	= plate displacement components
x,y	= plate coordinates
λ	= $2qa^3/MD_x$
μ	= $\rho a/\rho_m h$
ν	= Poisson's ratio
δ	= virtual operator
ρ	= air density
ρ_m	= plate density
σ,ε	= stress, strain
ω,ω_n	= frequency, nth natural
$\psi;\psi_m$	= yaw angle of flow; modal shape function

Subscripts

f	= flutter
s	= support
x,y	= component directions

Superscripts

$(\cdot)$	= $\partial/\partial +$

Introduction

PREVIOUS discussions of space shuttle panel flutter problems are available in Refs. 1 and 2. The present work is directed toward a more accurate structural modeling of a class of metallic reradiative thermal protection systems proposed for space shuttle and other high supersonic and hypersonic flight vehicles. For such TPS panels, point spatial supports are inherent to the design. Earlier studies[1,2] have dealt with simpler panel support conditions.

Received July 21, 1972; revision received January 19, 1973. A preliminary version of this work was reported in Paper 72-350, presented at the AIAA/ASME/SAE 13th Structures, Structural Dynamics and Materials Conference, San Antonio, Texas, April 10–12, 1972. It has been supported by NASA Grant NGR 31-001-146, NASA Langley Research Center, Hampton, Va.

Index categories: Aeroelasticity and Hydroelasticity; Structural Dynamic Analysis.

* Professor, Department of Aerospace and Mechanical Sciences. Member AIAA.

Analysis

Rayleigh-Ritz Approach

In the linear approximation one may formulate a rather general theoretical panel model which is valid for arbitrary structural shapes, support conditions, and stiffness distributions (orthotropicity). Perhaps the most economical and informative way to approach the problem is to employ an energy approach with Hamilton's Principle. Considering for definiteness a flat plate we may write the elastic potential energy (using rectangular Cartesian coordinates)

$$U=\frac{1}{2}\iint\left[D_x\left(\frac{\partial^2 w}{\partial x^2}\right)^2+D_y\left(\frac{\partial^2 w}{\partial y^2}\right)^2+2D_1\frac{\partial^2 w}{\partial x^2}\frac{\partial^2 w}{\partial y^2}+4D_{xy}\left(\frac{\partial^2 w}{\partial x\partial y}\right)^2\right]dxdy \quad (1)$$

where for an isotropic plate

$$D_x=D_y=D$$
$$D_1=\nu D$$
$$D_{xy}=[(1-\nu)/2]D$$

the kinetic energy

$$T=\tfrac{1}{2}\iint m(\partial w/\partial t)^2\,dxdy \quad (2)$$

and the virtual work done by the pressure distribution

$$\delta W=-\iint p\delta w dxdy \quad (3)$$

Hamilton's Principle may be stated as

$$\delta\int(T-U)dt+\int\delta W dt=0 \quad (4)$$

Applying the variational or virtual operator δ we may derive the Euler-Lagrange equation of equilibrium and associated boundary conditions. However, it is generally preferable to proceed by using a Rayleigh-Ritz approximation starting from the energy and work relations directly.

Expanding the plate deflection as

$$w=\sum_m q_m(t)\psi_m(x,y) \quad (5)$$

and substituting into Eqs. (1–3) we have

$$U=\tfrac{1}{2}\sum_m\sum_n K_{mn}q_m q_n \quad (6)$$

$$T = \tfrac{1}{2}\sum_m \sum_n M_{mn}\dot{q}_m\dot{q}_n \tag{7}$$

$$\delta W = -\sum_n Q_n \delta q_n \tag{8}$$

where

$$K_{mn} = \iint \left[D_x \frac{\partial^2\psi_m}{\partial x^2}\frac{\partial^2\psi_n}{\partial x^2} + 2D_1 \frac{\partial^2\psi_m}{\partial x^2}\frac{\partial^2\psi_n}{\partial y^2} + D_y \frac{\partial^2\psi_m}{\partial y^2}\frac{\partial^2\psi_n}{\partial y^2} + 4D_{xy}\frac{\partial^2\psi_m}{\partial x\partial y}\frac{\partial^2\psi_n}{\partial x\partial y}\right] dxdy \tag{9}$$

$$M_{mn} \equiv \iint m\psi_n\psi_m dxdy \tag{10}$$

$$Q_n \equiv \iiint p\psi_n dxdy \tag{11}$$

The Euler-Lagrange or simply Lagrange's equations are

$$\sum_m M_{mn}\ddot{q}_m + \sum_m \tilde{K}_{mn}q_m + Q_n = 0 \tag{12}$$

where

$$\tilde{K}_{mn} \equiv \tfrac{1}{2}[K_{mn} + K_{nm}]$$

Note K_{mn} is not necessarily a symmetric matrix but $\tilde{K}_{mn}$ is. Earlier results presented in the preprint were in error due to use of K_{mn} rather than $\tilde{K}_{mn}$.

The essential advantage of the Rayleigh-Ritz approach over Galerkin's method is the choice of functions ψ_m. In Galerkin's method all boundary conditions must be satisfied by each ψ_m; in the Rayleigh-Ritz approach only the geometric boundary conditions need be satisfied by each ψ_m. In fact, as we shall discuss below, one can modify the method so that the ψ_m need not satisfy any of the boundary or support conditions.

Equation (12) can be simplified significantly if we are so fortunate as to know and use the panel modes. Then

$$M_{mn} = M_n\delta_{mn};\ \tilde{K}_{mn} = \omega_n{}^2 M_n\delta_{mn}$$

and we have

$$M_n[\ddot{q}_n + \omega_n{}^2 q_n] + Q_n = 0 \tag{13}$$

Of course, by considering Eq. (12) for $Q_n = 0$ we can determine the eigenfunctions as a linear combination of any set of admissible primitive functions ψ_m by solving the eigenvalue problem

$$(-\omega^2[M_{mn}] + [\tilde{K}_{mn}])\{q_n\} = \{0\} \tag{14}$$

Other techniques could be used for determining the eigenmodes such as the finite element or finite difference methods. For odd shaped panels, in particular, such methods may be advantageous for first determining the natural modes. See discussion of Ref. 3.

Arbitrary Support Conditions

Finally, let us consider a modification to the Rayleigh-Ritz method which allows one to use a single modal expansion for any support condition, thereby eliminating one of the principle practical disadvantages of the modal expansion approach. We shall distinguish between elastic supports and rigid supports; surprisingly perhaps, the former is conceptually easier to handle than the latter. For example, consider a point translational spring support with stiffness K_T, at some point x_s,y_s. The associated elastic energy is

$$\tfrac{1}{2}K_T w^2(x_s,y_s) \tag{15}$$

which leads to an added term to the generalized stiffness of the form

$$K_{mn} = \cdots + K_T\psi_m(x_s,y_s)\psi_n(x_s,y_s) \tag{16}$$

By allowing $K_T \to \infty$, one may obtain a rigid support; other types of stiffness or mass supports may similarly be taken into account and by using several point supports a line support condition may also be approximated.

There may be a practical difficulty with taking the limit as $K_T \to \infty$ or similar limits as the corresponding stiffness terms create numerical difficulties due to small differences between large numbers. This can be overcome by careful numerical work but an alternative, more efficient, and possibly more elegant approach is available using Lagrange multipliers and appropriate constraint relations. For example, consider a rigid translational support at points x_s,y_s. The constraint conditions are

$$w(x_s,y_s) = \sum q_m\psi_m(x_s,y_s) = 0 \qquad s = 1, \ldots, S \tag{17}$$

The Lagrangian, $L \equiv T - U$, is modified to read

$$L \equiv T - U + \sum_s \lambda_s \sum q_m\psi_m(x_s,y_s) \tag{18}$$

and Lagrange's equations become

$$(d/dt)(\partial L/\partial\dot{q}_m) - \partial L/\partial q_m + Q_m = 0 \qquad m = 1, \ldots, M \tag{19}$$

$$\partial L/\partial\lambda_s = 0 \qquad s = 1, \ldots, S \tag{20}$$

Equation (20) simply reproduces Eqs. (17), of course. Equations (19) and (20) are $M + S$ equations for the M, q_m, plus S, λ_s, unknowns.

In solving these equations by step-by-step temporal integration (as we shall do subsequently) one must use the fact that Eqs. (17) constrain the modal velocities $\dot{q}_m$ and accelerations $\ddot{q}_m$ as follows:

$$\dot{w}(x_s,y_s) = \sum_m \dot{q}_m\psi_m(x_s,y_s)\} = 0 \tag{21}$$

$$\ddot{w}(x_s,y_s) = \sum_m \ddot{q}_m\psi_m(x_s,y_s) = 0 \qquad s = 1, \ldots, S \tag{22}$$

Hence, one can only specify initial conditions on M-S of the $\dot{q}_m$ and q_m solving for the remaining S from Eqs. (17) [or (20)] and (21). One may then solve for all of the M, $\ddot{q}_m$, and S, λ_s, from Eqs. (19) and (22). With this information one may project to the next time step using any of the standard numerical integration methods and obtain a time history of the plate motion. For a discussion of natural modes and frequencies see Refs. 4 and 5.

Aerodynamic Forces

In determining the (aerodynamic) generalized forces we normally include both the prescribed external forces such as those due to acoustic sources as well as aerodynamic forces due to the panel motion itself. Only the latter are important from the standpoint of flutter per se and in the usual acoustic response analysis only the former are included. It has been pointed out however that from the standpoint of determining total panel response both must sometimes be included.[6] Here we shall neglect the external acoustic excitation forces (though they are readily incorporated into the analysis) since information on their time histories and spatial distribution is lacking. We shall concentrate instead on the motion dependent aerodynamic forces and their effect on panel flutter. Any of the available levels of aerodynamic theory may be incorporated into the present analysis, see Ref. 7. For the present we shall use the simplest available theory, the so-called "piston" or two-dimensional quasi-steady theory where the aerodynamic pressure is given by

$$p = (2q/M)[\partial w/\partial x + (1/U)\partial w/\partial t] \tag{23}$$

This is easily modified to include yaw angle effects.[2]

Using Eqs. (5) and (23) in Eq. (3), we may determine the generalized forces required in Eqs. (8, 12, and 19)

$$Q_n = \frac{2q}{M}\left\{\sum_m q_m \iint \frac{\partial \psi_m}{\partial x}\psi_n dxdy + \frac{\dot{q}_m}{U}\iint \psi_m \psi_n dxdy\right\} \quad (24)$$

Similar but more complicated results are available for the other aerodynamic theories.[7,8]

Nonlinear Stiffnesses

If one wishes to examine the post-flutter behavior of a panel or the onset of flutter for a panel which is pressurized or buckled, then the nonlinear structural stiffness must be included in the theoretical model.[7] Physically this nonlinear stiffness arises from the tension induced by stretching as the panel bends out of its undeformed plane. The appropriate mathematical description is the nonlinear plate theory due to von Kármán. The potential energy of the plate is that given by Eq. (1), the bending energy, plus the stretching energy given below (for simplicity we consider an isotropic panel)[9]

$$U_s = \frac{Eh}{2(1-\nu^2)}\iint\left\{\left[\frac{\partial u}{\partial x}+\frac{1}{2}\left(\frac{\partial w}{\partial x}\right)^2\right]^2 + \left[\frac{\partial v}{\partial y}+\frac{1}{2}\frac{\partial w}{\partial y}\right)^2\Big]^2 + 2\nu\left[\frac{\partial u}{\partial x}+\frac{1}{2}\left(\frac{\partial w}{\partial x}\right)^2\right]\left[\frac{\partial v}{\partial y}+\frac{1}{2}\left(\frac{\partial w}{\partial y}\right)^2\right] + \frac{(1-\nu)}{2}\left[\frac{\partial v}{\partial x}+\frac{\partial u}{\partial y}+\frac{\partial w}{\partial x}\frac{\partial w}{\partial y}\right]^2\right\}dxdy \quad (25)$$

At this point we have two alternatives. Treat the problem using suitable modal expansions for u, v, and w or do some further analysis to develop a variational formulation in terms of w and an Airy stress function. The latter is more convenient if we assume the supports provide no in-plane restraint. It is also more nearly representative of applications.

Taking the variation with respect to w and using the stress strain, strain-displacement and stress-resultant definitions given below

$$\begin{aligned}
\sigma_{xx} &= [E/(1-\nu^2)][\varepsilon_{xx}+\nu\varepsilon_{yy}]\\
\sigma_{yy} &= [E/(1-\nu^2)][\varepsilon_{yy}+\nu\varepsilon_{xx}]\\
\sigma_{xy} &= [E/2(1+\nu)]\varepsilon_{xy}\\
\varepsilon_{xx} &= \partial u/\partial x + \tfrac{1}{2}(\partial w/\partial x)^2\\
\varepsilon_{yy} &= \partial v/\partial y + \tfrac{1}{2}(\partial w/\partial y)^2\\
\varepsilon_{xy} &= \partial u/\partial y + \partial v/\partial x + (\partial w/\partial x)(\partial w/\partial y)\\
N_{xx} &\equiv \sigma_{xx}h, \quad N_{yy} \equiv \sigma_{yy}h, \quad N_{xy} \equiv \sigma_{xy}h,
\end{aligned} \quad (26)$$

we obtain

$$\delta U_s = \iint\left[N_{xx}\frac{1}{2}\delta\left(\frac{\partial w}{\partial x}\right)^2 + N_{yy}\frac{1}{2}\delta\left(\frac{\partial w}{\partial y}\right)^2 + N_{xy}\delta\frac{\partial w}{\partial x}\frac{\partial w}{\partial y}\right]dxdy \quad (27)$$

This is the result we will need for Hamiltons Principle.

By taking variations with respect to u and v, we may develop two equations of equilibrium for u and v. These are satisfied identically by introducing an Airy stress function F

$$N_{xx} \equiv \partial^2 F/\partial y^2, \quad N_{yy} \equiv \partial^2 F/\partial x^2, \quad N_{xy} \equiv -\partial^2 F/\partial x \partial y \quad (28)$$

F and w are further related by a strain compatibility relation[9]

$$\nabla^4 F/Eh = (\partial^2 w/\partial x\partial y)^2 - (\partial^2 w/\partial x^2)\partial^2 w/\partial y^2 \quad (29)$$

Expanding F,

$$F = \sum_k A_k F_k(x,y) \quad (30)$$

and using the previous expansion for w, Eq. (5), we can obtain a Galerkin solution for Eq. (29)

$$\sum_k A_k S1_{kl} = \sum_m \sum_n q_m q_n S2_{mnl} \quad (31)$$

From Eq. (27), using Eqs. (5, 28 and 30),

$$\delta U_s = \sum_m \sum_n \left(\sum_k S_{mnk}A_k\right)\delta\frac{q_m q_n}{2} \quad (32)$$

where

$$S_{mnk} \equiv \iint\left\{\frac{\partial^2 F_k}{\partial y^2}\frac{\partial \psi_m}{\partial x}\frac{\partial \psi_n}{\partial x} + \frac{\partial^2 F_k}{\partial x^2}\frac{\partial \psi_m}{\partial y}\frac{\partial \psi_n}{\partial y} - 2\frac{\partial^2 F_k}{\partial x 2y}\frac{\partial \psi_m}{\partial x}\frac{\partial \psi_n}{\partial y}\right\}dxdy \quad (33)$$

$$S1_{kl} \equiv \iint\frac{(\nabla^4 F_k)}{Eh}F_l dxdy$$

$$S2_{mnl} \equiv \iint\left[\frac{\partial^2 \psi_m}{\partial x\partial y}\frac{\partial^2 \psi_n}{\partial x\partial y} - \frac{\partial^2 \psi_m}{\partial x^2}\frac{\partial^2 \psi_n}{\partial y^2}\right]F_l dxdy$$

For zero-stress edge conditions, $F = \partial F/\partial x = 0$ on $x = \text{const}$, etc., one can show that

$$S_{mnk} = 2\,S2_{mnk} \quad (34)$$

by a suitable integration by parts. The nonlinear stiffness is defined as the coefficient of the double summation in Eq. (32)

$$K_{mn}^{\text{Nonlin}} \equiv \sum_k S_{mnk}A_k \quad (35)$$

where A_k is known in terms of q_m from Eq. (31). Hence in Eq. (12) we supplement the linear stiffness, K_{mn}, with the nonlinear stiffness from Eq. (35) [and (31)] and proceed to obtain time histories of the panel motion using the same method as discussed previously for the linear case. K_{nm}^{Nonlin} must be symmetricized as was its linear counterpart, of course.

Results

Natural Frequencies and Flutter Boundaries for Point Supported Orthotropic Plates

Effect of support position

We consider a square plate with four symmetrically placed rigid supports along the panel diagonals.

In Fig. 1 natural frequencies for the lower plate modes are shown as a function of support position from plate center, $x_s/(a/2) = 0$ to plate corner, $x_s/(a/2) = 1.0$. In Fig. 2 the flutter boundary is presented. Note that as the supports approach the center the panel undergoes static divergence or zero frequency flutter. As $x_s/(a/2) \to 0$, the plate is essentially clamped at its center and its flutter behavior is similar to the leading-edge divergence of a wing with a clamped trailing edge.

Next we consider a one-dimensional plate (beam) simply supported at two points. The rearward support is fixed at the trailing edge; the forward support is systematically varied from leading edge to trailing edge. In Fig. 3 the flutter dynamic pressure is plotted vs forward support position, x_s/a. For $x_s/a \to 0$ we have the well-known result for a plate pinned at its leading and trailing edges.[7] As $x_s/a \to 1$ we obtain another well-known result due to Biot[10] for the divergence (zero frequency flutter) of a beam clamped at its trailing edge. The most interesting result is the relatively small distance the forward support need be moved rearward in order for the instability to change from flutter to divergence with a corresponding dramatic decrease in the dynamic pressure at which an instability occurs.

Effect of length to width ratio

In Fig. 4 the fundamental natural frequency is shown for several length to width ratios a/b. The largest frequency

occurs when the supports are at a nodal point of the lowest frequency (nonzero) free-free plate mode. For $a/b \ll 1$ or $\gg 1$ the plate behaves as a simply supported beam as far as the fundamental mode is concerned. In Fig. 5 the corresponding flutter boundary is given. For $a/b \gg 1$ the result approaches that of simply supported beam. For $a/b \ll 1$ no such simple limit exists. Moreover the results for small a/b are sensitive to small mass unbalance. Placing a small mass aft of mid-chord drops the flutter boundary precipitously.

Effect of yaw flow angle

For panels with one direction much stiffer than the other, the flow directed along the stiffer direction will give a much higher flutter dynamic pressure. However if the flow is slightly yawed the flutter dynamic pressure will rapidly fall toward the lower flutter dynamic pressure associated with the flow in the less stiff direction. In Fig. 6 the flutter dynamic pressure is plotted vs yaw angle for a typical point supported panel. Clearly point supported panels are affected by yaw angle in a manner similar to their more conventionally supported counterparts.[2,11]

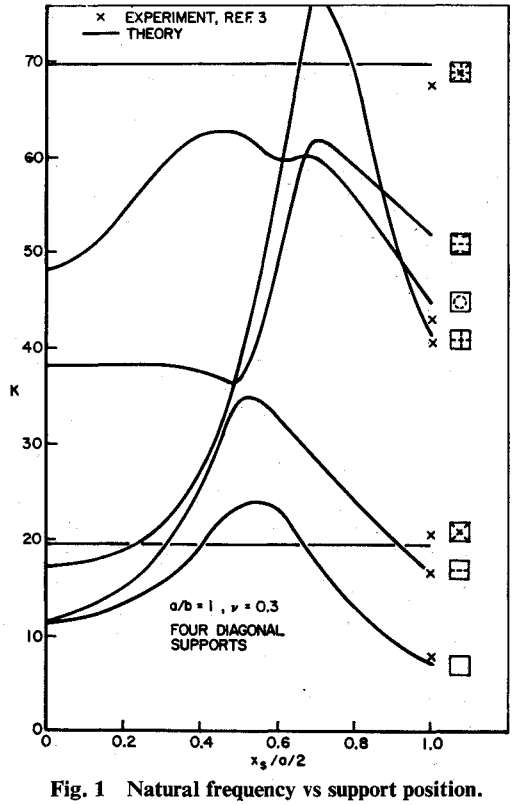

Fig. 1 Natural frequency vs support position.

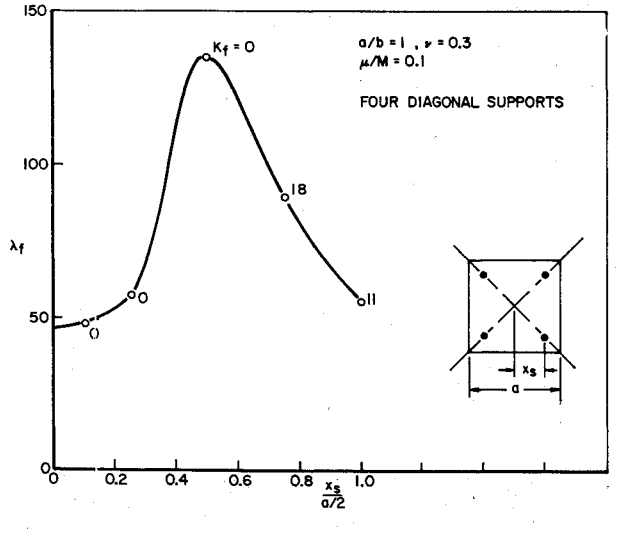

Fig. 2 Flutter dynamic pressure vs support position.

Typical space shuttle panel

It is perhaps somewhat presumptuous to discuss a "typical" space shuttle panel. However a number of designs have been proposed and we shall analyze one such which has been studied at the NASA Langley Research Center. It is a curved iso-

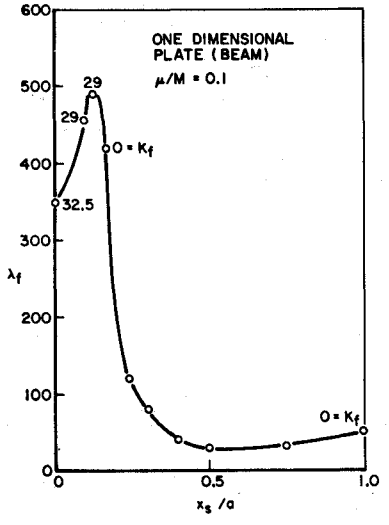

Fig. 3 Flutter dynamic pressure vs forward support position.

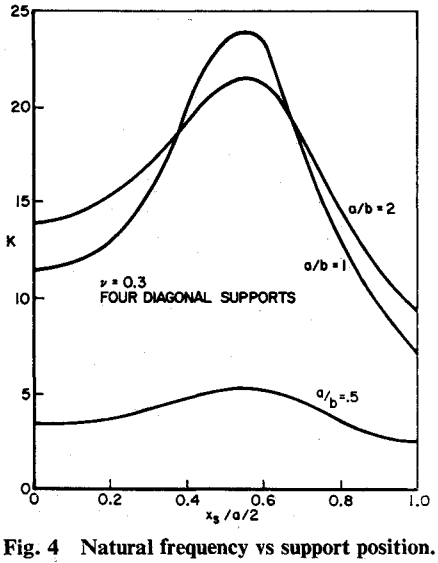

Fig. 4 Natural frequency vs support position.

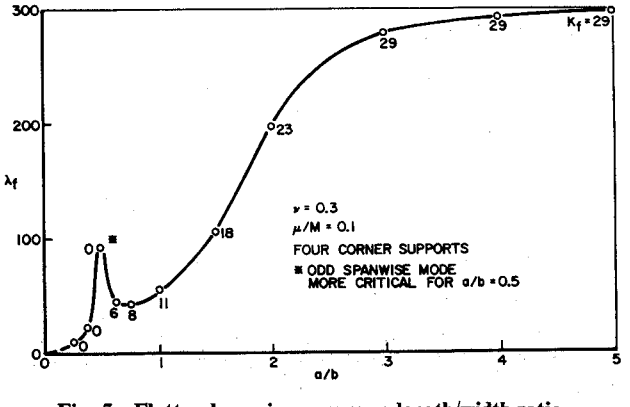

Fig. 5 Flutter dynamic pressure vs length/width ratio.

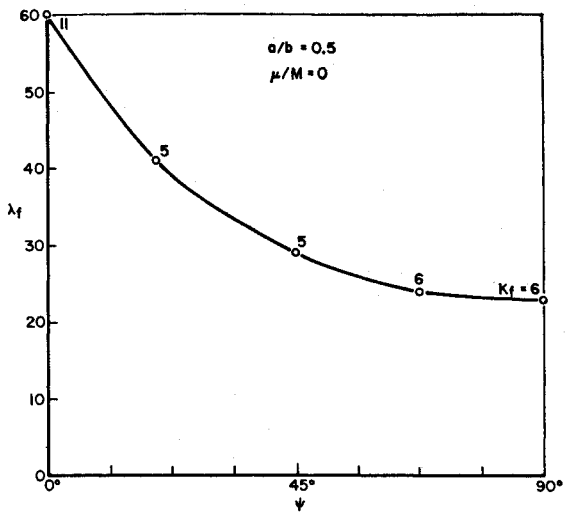

Fig. 6 Flutter dynamic pressure vs angle of yaw. Isotropic plate.

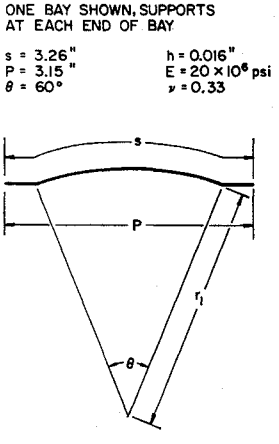

Fig. 7 Typical space shuttle design.

tropic plate on point supports which we shall model as a flat orthotropic plate using the method of Ref. 12. The pertinent dimensions are shown in Fig. 7. The orthotropic plate stiffnesses are

$$D_x = 7.661 \text{ in.-lb},\ D_y/D_x = 739,\ D_1/D_x = 0.15,\ D_{xy} = 0.35$$

$a/b = 3$, and there are fourteen equally-spaced point supports along each of the side edges. It is of interest to determine whether such a panel can be analyzed as having a continuous simply supported side edge. In Fig. 8 the flutter dynamic pressure parameter (based on constant panel length) is plotted vs number of equally spaced supports N. As $N \to \infty$ the continuous support condition is approach. Note however that for $N = 14$ the result is still substantially different from $N \to \infty$. The general shape of the curve, which may at first appear surprising, can be better understood by recalling that for small N we are dealing with essentially a multibay beam-like structure. It is known that for such structures $\lambda_f \sim (N-1)^3$ (see Ref. 13). Hence for small N there is a rapid increase in λ_f which reaches a maximum and then begins to decrease for large N. An alternative method of approaching the same limit is to fix the dimensions of one bay and systematically increase the number of bays and hence number of supports and a/b. Such results are shown in Fig. 9 where all quantities are nondimensionalized by plate width. As expected flutter dynamic pressure decreases with increasing number of bays.

We have also evaluated the effect of flow yaw angle for a two-bay (three-support) model of such a panel. The results

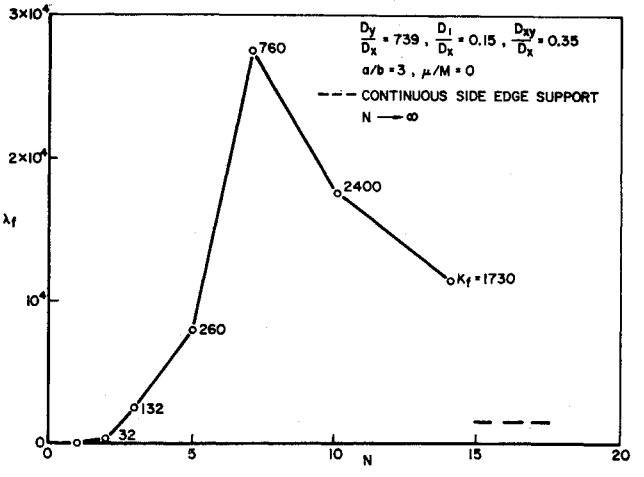

Fig. 8 Flutter dynamic pressure vs number of supports. Constant length.

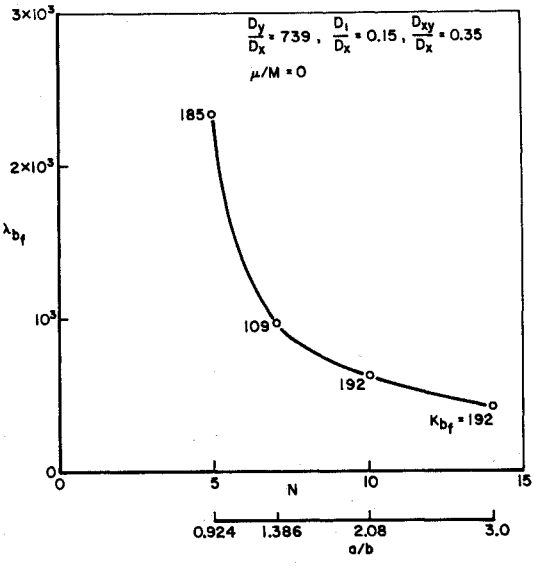

Fig. 9 Flutter dynamic pressure vs number of supports. Constant width.

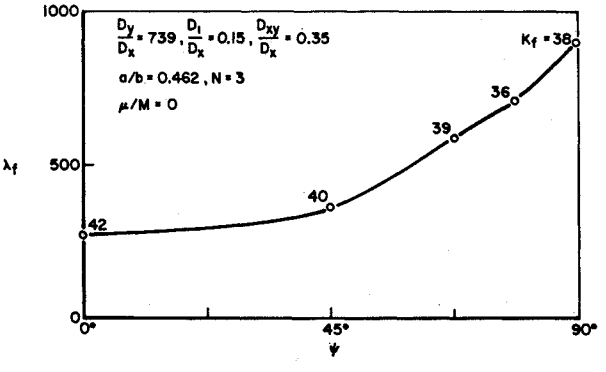

Fig. 10 Flutter dynamics pressure vs angle of yaw. Orthotropic plate.

are shown in Fig. 10. For small ψ, $\lambda_f \sim (\cos\psi)^{-1}$. Multibay panels (or at least this one) do not seem to behave substantially different with yaw angle than single-bay panels.[2,11] As expected, adding bays in the streamwise direction has a much greater effect (see Fig. 9) than adding spanwise bays.

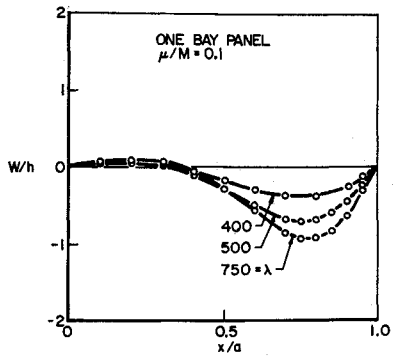

Fig. 11 Flutter deformation mode shape. One bay panel.

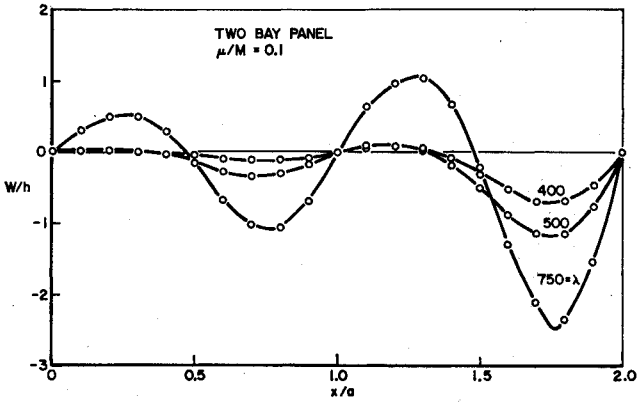

Fig. 12 Flutter deformation mode shape. Two bay panel.

Post Flutter Behavior

We first consider a one-dimensional plate. In Figs. 11 and 12 the deformation shape of the plate at the maximum response during its limit cycle oscillation is given. Figure 11 presents results for a plate simply supported at its leading and trailing edges. Figure 12 presents results for a plate twice as long with supports at leading edge, midchord and trailing edge, i.e., a "two-bay panel." It is known that according to linear theory the flutter dynamic pressure is the same for "one-bay" and "two-bay" panels (for equal bay length).[13] Moreover, such theory predicts that the flutter deformation shape is the same in both bays of the two-bay panel (the second bay amplitude being roughly five times the first bay) and also the same as that for a one-bay panel. Of course, the linear theory cannot give any information about the absolute amplitude of the panel during flutter. The present nonlinear results show that the flutter amplitude in the second bay of the two-bay panel is substantially greater than that of the one-bay panel. In all the aforementioned results the supports are assumed to provide complete in-plane restraint at the leading and trailing edges only.

For the other example of post-flutter behavior we return to a rectangular panel with four corner supports. In Figs. 13 results are given for peak flutter amplitude vs dynamic pressure for $a/b = 0.5$, 1.0, 2.0, and 4.0. For $a/b = 0.5$, of course, the results are for a statically diverged panel near λ_f. However, for sufficiently large λ, the panel oscillates about a static equilibrium position, as indicated by the vertical bars.

The significant, but unsurprising, finding is that the flutter limit cycle amplitudes for such plates are much larger than those of a plate on continuous supports. Indeed those plates would probably fail catastrophically if the flutter regime were penetrated to any substantial degree. On the other hand, as the number of point supports increased one would expect the postflutter limit cycle behavior to more nearly resemble that of a continuously supported plate. In all of the preceding

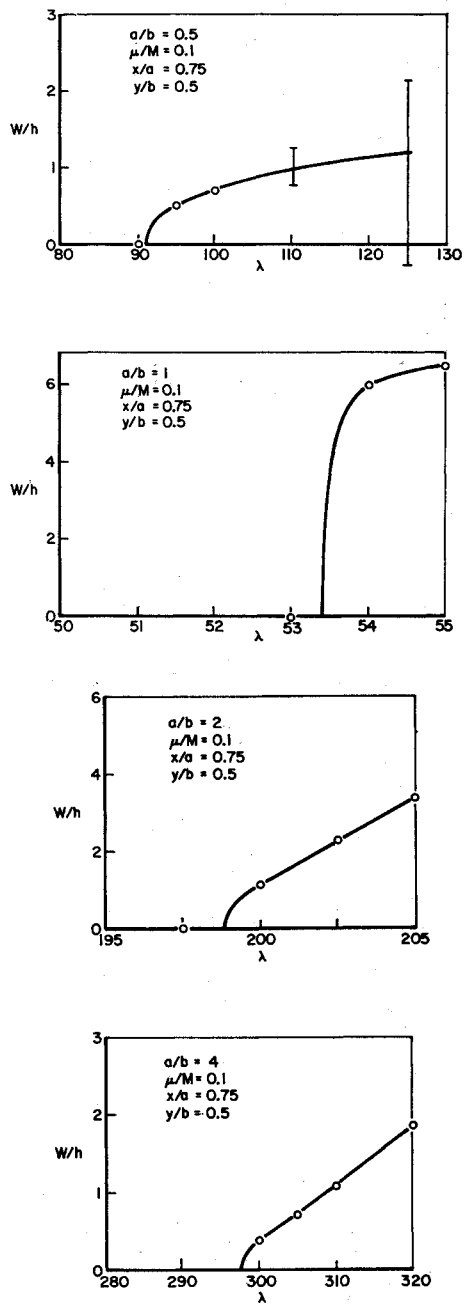

Fig. 13 Peak flutter amplitude vs dynamic pressure.

results the supports are assumed to provide zero in-plane restraint.

Summary and Conclusions

A structural analysis has been developed for orthotropic, point-supported rectangular panels. Natural frequencies, flutter boundaries and post-flutter behavior have been determined, the latter using quasi-steady aerodynamic theory including yaw angle effects. Several interesting results are obtained. 1) Under certain circumstances such panels may diverge rather than flutter. 2) The effect of yaw angle is similar to that for conventionally supported panels. 3) An example of a typical space shuttle panel design indicates that even for a large number of panel point supports the discreteness of the supports may be important. 4) The post-flutter limit cycle amplitudes for point supported plates are substantially larger than the corresponding results for continuously supported plates.

References

[1] Gaspers, P. A., Jr., "Applications of Recent Panel Flutter Research to Space Shuttle. Part I—Boundary Layer and Hypersonic Effects," *NASA Space Shuttle and Technology Conference, Vol. III—Dynamics and Aeroelasticity*, TM X-2274, 1971, NASA, pp. 247–264.

[2] Bohon, H. L. and Shore, C. P., "Applications of Recent Panel Flutter Research to Space Shuttle. Part II—Influence of Edge Clips and Flow Angularity," TM X-2274, March 1971, NASA, pp. 247–264.

[3] Leissa, A., *Vibration of Plates*, NASA SP-160, 1969.

[4] Dowell, E. H., "Free Vibrations of a Linear Structure with Arbitrary Support Conditions," *Journal of Applied Mechanics*, Vol. 38. No. 3, Sept. 1971, pp. 595–600.

[5] Dowell, E. H., "Free Vibrations of an Arbitrary Structure in Terms of Component Modes," *Journal of Applied Mechanics*, Vol. 39, No. 3, Sept. 1972, pp. 727–732.

[6] Dowell, E. H., "Noise or Flutter or Both?" *Journal of Sound and Vibration*, Vol. 11, No. 2, 1970, pp. 159–180.

[7] Dowell, E. H., "Panel Flutter: A Review of the Aeroelastic Stability of Plates and Shells," *AIAA Journal*, Vol. 8, No. 3, March 1970, pp. 385–399.

[8] Dowell, E. H., "Generalized Aerodynamic Forces on a Plate Undergoing Transient Motion in a Shear Flow with an Application to Panel Flutter," *AIAA Journal*, Vol. 9, No. 5, May 1971, pp. 834–841.

[9] Washizu, K., *Variational Methods in Elasticity and Plasticity*, Pergamon Press, New York, 1968, pp. 163–165.

[10] Bisplinghoff, R. L., Ashley, H., and Halfman, R., *Aeroelasticity*, Addison-Wesley, Reading, Mass., 1955.

[11] Gaspers, P. A., Jr. and Redd, B., "A Theoretical Analysis of the Flutter of Orthotropic Panels Exposed to a High Supersonic Stream of Arbitrary Direction," TN D-3551, 1966, NASA.

[12] Stroud, W. J., "Elastic Constants for Bending and Twisting of Corrugation-Stiffened Panels," TR-166, 1963, NASA.

[13] Dowell, E. H., "Flutter of Multibay Panels at High Supersonic Speeds," *AIAA Journal*, Vol. 2, No. 10, Oct. 1964, pp. 1805–1811

JUNE 1973 J. SPACECRAFT VOL. 10, NO. 6

A Theoretical and Experimental Study of a Jet Stretcher System

R. C. BAUER,* E. H. MATKINS,† R. L. BAREBO,† AND W. C. ARMSTRONG‡

ARO Inc. Arnold Air Force Station, Tenn.

Analytical techniques were developed for estimating diffuser performance, and for evaluating the feasibility of using an axisymmetric jet stretcher for angle-of-attack testing. Diffuser starting limits are imposed by : 1) nozzle exit boundary layer, 2) blockage area, and 3) jet stretcher ambient pressure level. The diffuser analysis estimates the starting conditions limited by either the nozzle exit boundary layer or the jet stretcher ambient pressure level. Experimental results show the analysis for diffuser starting conditions to be conservative and accurate to within 10% for engine-off operation. The feasibility of using an axisymmetric jet stretcher for angle-of-attack testing was determined by establishing a criteria for acceptable jet stretcher performance based on maintaining the static pressure distribution on the test body to within ± 10% of the interference free pressure distribution. A local application of linearized theory was used to determine the proper position of the jet stretcher and to indicate the regions that require bleed flow. The analysis was applied to a small-scale jet stretcher system for test body angles of attack of 4° and 8°. Experimental results verified the analysis and showed that the maximum possible off-design angle of attack of the test body is about 5.0°

Nomenclature

A = area
C_p = model pressure coefficient
cp = specific heat at constant pressure
F = stream thrust plus pressure force
F_s = total drag force
L = diffuser gap, see Fig. 1
l = length of cylindrical diffuser, see Fig. 1
M = Mach number
m = mass flow
p = static pressure
q = dynamic pressure
r_N = radius of nozzle exit
r_j = radius of jet stretcher inlet
T = static temperature
X_B = distance from nose of test body along its centerline
X_F = feedback distance
X_{FA} = allowable feedback distance, see Fig. 3
X_{js} = distance from nozzle exit to jet stretcher inlet, see Fig. 3
X_j = distance from jet stretcher inlet along its centerline
α_B = angle of test body relative to nozzle centerline; angle of attack, see Fig. 14
α_j = angle of jet stretcher relative to nozzle centerline, see Fig. 14
β = mismatch angle between jet stretcher surface and the interference free flowfield, deg, see Fig. 14
γ = ratio of specific heats
δ_N = total boundary-layer thickness at nozzle exit
θ = radial angle measured from leeward side of test body, deg
λ = blockage ratio—open area between inlets to annular area upstream of inlets
μ = Mach angle

Subscripts

B = diffuser exit, see Fig. 1
BLS = Boundary-layer separation

Received September 12, 1972; presented as Paper 72–1024 at the AIAA 7th Aerodynamic Testing Conference, Palo Alto, Calif., September 13–15, 1972; revision received February 5, 1973. This research was supported by the Arnold Engineering Development Center, under sponsorship of the Aerospace Propulsion Laboratory.

Index category: Airbreathing Engine Testing.

* Research Engineer. Member AIAA.

† Project Engineer.

‡ Scientist.